THE JOURNAL OF BIOLOGICAL CHEMISTRY VOL. 282, NO. 16, pp. 12104–12111, April 20, 2007

Granzyme K Directly Processes Bid to Release Cytochrome *c* and Endonuclease G Leading to Mitochondria-dependent Cell Death*

Received for publication, November 29, 2006, and in revised form, January 16, 2007 Published, JBC Papers in Press, February 16, 2007, DOI 10.1074/jbc.M611006200

Tongbiao Zhao[1], **Honglian Zhang**[1], **Yuming Guo, and Zusen Fan**[2]

From the National Laboratory of Biomacromolecules and Center for Infection and Immunity, Institute of Biophysics, Chinese Academy of Sciences, 15 Datun Road, Beijing 100101, China

Granule-mediated cytolysis is the major pathway for killer lymphocytes to kill pathogens and tumor cells. Little is known about how granzyme K functions in killer lymphocyte-mediated cytolysis. We previously showed that human GzmK triggers rapid cell death independently of caspase activation with single-stranded DNA nicks, similar to GzmA. In this study we found that GzmK can induce rapid reactive oxygen species generation and collapse of mitochondrial inner membrane potential (ΔΨm). Blockade of reactive oxygen species production by antioxidant *N*-acetylcysteine or superoxide scavenger Tiron inhibits GzmK-induced cell death. Moreover GzmK targets mitochondria by cleaving Bid to generate its active form tBid, which disrupts the outer mitochondrial membrane leading to the release of cytochrome *c* and endonuclease G. Thus, we showed herein that GzmK-induced caspase-independent death occurs through Bid-dependent mitochondrial damage that is different from GzmA.

Granzyme K (GzmK)[3] was originally discovered as a second tryptase among all the granzymes (1). GzmK is closely linked together with the other tryptase GzmA on the same chromosome both in mice and humans (2, 3). Tryptase is essential for cytotoxic T lymphocyte (CTL)-mediated cytolysis (4). GzmA-deficient CTLs have only slightly reduced cytolytic activity against allogeneic targets, which still contain 20% tryptase activity (5). GzmA-deficient CTLs do not affect GzmK gene and its expression. It suggests tryptase GzmK might be a potent granzyme to rescue GzmA function. GzmK is less abundant than GzmA and -B in human lymphokine-activated killer cells (1). However GzmK expresses at high levels in CD56^{high} NK cells, memory CD8+ T cells, and CD56+ T cells (6). A recent report showed that circulating levels of GzmK are significantly elevated in virus-infected patients (7). It suggests GzmK may play an important role in cytolytic lymphocyte-mediated viral clearance.

It is unclear how GzmK functions in cytolytic lymphocyte-mediated cytotoxicity. One early report showed rat GzmK is a slow acting enzyme to induce DNA fragmentation without apoptotic nuclear morphology (8). We found human GzmK induces a rapid death with single-stranded DNA nicks independently of caspase activation (9). MacDonald *et al.* (10) showed that rat GzmK abolishes mitochondrial membrane potential (ΔΨ) and induces reactive oxygen species (ROS) production without release of cytochrome *c* (cyt *c*). Mitochondria play a central role in apoptosis. Undergoing apoptosis, mitochondrial function is completely disrupted by loss of ΔΨ and an increase of ROS. The outer mitochondrial membrane is destroyed, causing the release of proapoptotic factors, such as cyt *c*, endonuclease G (EndoG), high temperature-requirement protein A2, SMAC, and apoptosis-inducing factor (AIF), which can initiate caspase activation and/or other apoptotic process (11, 12). The release of the proapoptotic factors from mitochondria is triggered by the opening of a high conductance channel, the permeability transition pore (PTP), which initiates an increase of inner membrane permeability leading to proapoptotic factors release to the intermembrane space (13). ROS induce the opening of the PTP through oxidation-dependent mechanisms and are potent inducers of apoptosis (12). Translocation of proapoptotic proteins such as Bid and Bax from the cytosol to the outer mitochondrial membrane disrupts the outer membrane integrity (14).

One recent study showed GzmA induces a rapid accumulation of ROS and loss of ΔΨ in a caspase-independent manner (15). But GzmA does not cleave Bid or cause the release of proapoptotic factors (16, 17). In this study, we found GzmK provoked mitochondrial swelling and initiated loss of ΔΨ and rapid accumulation of ROS. Blockade of ROS by antioxidants or superoxide scavengers inhibited GzmK-induced cell death. GzmK directly degraded Bid and triggered release of cyt *c* and EndoG with a Bid-dependent way.

* This work was supported by The Hundred Talents Program of the Chinese Academy of Sciences (CAS) (to Z. F.), by grants from the National Natural Science Foundation of China Program (Grants 30500448 to T. Z. and 30470365 to Z. F., and the Outstanding Youth Grant 30525005 to Z. F.), and by Special Grants for President Scholarship and Innovation Study of CAS for outstanding graduate students, China Postdoctoral science Foundation, and K. C. Wong Education Foundation (Hong Kong) (to T. Z.). The costs of publication of this article were defrayed in part by the payment of page charges. This article must therefore be hereby marked "*advertisement*" in accordance with 18 U.S.C. Section 1734 solely to indicate this fact.

[1] Both authors contributed equally to this work.

[2] To whom correspondence should be addressed: Tel.: 86-10-6488-8457; Fax: 86-10-6487-1293; E-mail: fanz@moon.ibp.ac.cn.

[3] The abbreviations used are: GzmK, granzyme K; cyt *c*, cytochrome c; EndoG, endonuclease G; PFP, pore forming protein; PJ, Pro-Ject; Ad, adenovirus; ROS, reactive oxygen species; ΔΨm, mitochondrial inner membrane potential; $DIOC_6$, 3,3′-dihexyloxacarbocyanine iodide; HE, hydroethidine; CCCP, carbonyl cyanide *m*-chlorophenylhydrazone; CTL, cytotoxic T lymphocyte; SMAC, second mitochondria-derived activator of caspase; AIF, apoptosis-inducing factor; PTP, permeability transition pore; NAC, *N*-acetylcysteine; BSA, bovine serum albumin; FACS, fluorescence-activated cell sorting; Tiron, superoxide scavenger sodium 4,5-dihydroxybenzene 1,3-disulfonate; tBid, truncated Bid; rBid, recombinant Bid.

MATERIALS AND METHODS

Cell Lines, Antibodies, and Reagents—Cells were grown in RPMI 1640 (Jurkat) or Dulbecco's modified Eagle's medium (HeLa) supplemented with 10% fetal calf serum, 50 μM β-mercaptoethanol, and 100 μg/ml penicillin and streptomycin. Commercial antibodies were mouse monoclonal antibody against cyt *c* (BD Pharmingen), β-actin (Sigma-Aldrich), and CoxIV (Molecular Probes). Rabbit Bid and EndoG antisera were kindly gifts of Dr. X. Wang. $DIOC_6$ (3) and HE were from Molecular Probes (Eugene, OR). NAC and Tiron were from Sigma. The Pro-Ject™ (PJ) protein transfection reagent kit was from Pierce, and Annexin V-fluorescein isothiocyanate was from BD Pharmingen.

Loading GzmK with Pro-Ject, Adenovirus, or Perforin—Cells were washed three times in Hanks' balanced salt solution and resuspended in loading buffer (Hanks' balanced salt solution with 0.5 mg of BSA per ml, 1 mM $CaCl_2$, and 1 mM $MgCl_2$). HeLa cells or Jurkat cells (2×10^5) in 50 μl of loading buffer were incubated at 37 °C for the indicated times with different concentrations of GzmK, S-AGzmK, and/or an optimal dose of PJ, adenovirus (Ad), or perforin (PFP). Cells were incubated for an additional 15 min in 1 mM phenylmethylsulfonyl fluoride before being lysed for immunoblot.

Flow Cytometry Analysis—Fluorescein isothiocyanate-conjugated Annexin V was used to evaluate phosphatidylserine externalization. Target cells treated with S-AGzmK or GzmK plus PJ were stained with Annexin V-Fluos and propidium iodide and analyzed by flow cytometry using a FACSCalibur device (BD Biosciences). ROS production was performed by adding 2 μM HE just before flow cytometry analysis to cells treated for the indicated times and doses of GzmK plus adenovirus. 30-min exposure of cells to 3% H_2O_2 was used as a positive control. For $\Delta\Psi$m, cells treated with GzmK/Ad or CCCP were stained with $DiOC_6$ (3) and analyzed by flow cytometry as described previously (18). In brief, Jurkat cells treated with GzmK/Ad (100 pfu/ml) for the indicated times and doses were harvested and washed with Hanks' balanced salt solution three times. Cells were loaded with 20 nM $DiOC_6$ (3) for 5 min before FACS analysis. Cells treated with the membrane uncoupler CCCP were used as a positive control.

Transmission Electron Microscopy—HeLa cells (5×10^5) were treated with GzmK plus PJ at 37 °C for 4 h. After which, cells were washed twice and fixed with 2% glutaraldehyde at 4 °C for 1 h and postfixed with 2% osmium tetroxide. Cells were dehydrated with sequential immergence in 50%, 70%, 80%, 90%, and 100% ethanol, and then embedded in Spurr's resin. Ultrathin sections were mounted in copper grids and counterstained with uranyl acetate and lead citrate. Images were photographed and scanned by using the Eversmart Jazz+ program (Scitex).

Time-lapse Microscopy—HeLa cells were plated overnight in culture dishes in Dulbecco's modified Eagle's medium. The media were replaced with loading buffer (Hanks' balanced salt solution with 0.5 mg of BSA per ml, 1 mM $CaCl_2$, and 1 mM $MgCl_2$) plus 2′,7′-dichlorofluorescin diacetate (DCF-DA). The dishes remained at the 37 °C chamber before adding GzmK with adenovirus. Images were captured every 2 min.

Laser Scanning Confocal Microscopy—HeLa cells (4×10^4) grown overnight on Falcon culture slides (Molecular Probes) were stained with MitoTracker and washed twice with phosphate-buffered saline and then treated with GzmK plus PFP at 37 °C for 2 h. GzmB plus PFP was used as a positive control. After an additional wash with 1 mM phenylmethylsulfonyl fluoride, cells were fixed with 4% paraformaldehyde for 20 min at room temperature, permeabilized with 1% Triton X-100 for another 20 min, stained with anti-cyt *c* or anti-CoxIV or anti-EndoG antibodies, and then stained with the secondary antibody Alexa488-conjugated donkey anti-mouse IgG or Alexa594-conjugated donkey anti-rabbit IgG. The slides were mounted and observed using laser scanning confocal microscopy (Olympus FV500 microscope).

Bid Cleavage Assay—rBid or cell lysates (2×10^5 cell equivalents) were incubated at 37 °C for the indicated times with different concentrations of GzmK, S-AGzmK, or GzmB in 20-μl cleavage buffer (50 mM Tris-HCl, pH 7.5, 1 mM $CaCl_2$, 1 mM $MgCl_2$). The reaction products were boiled in SDS loading buffer before SDS-PAGE. For *in vivo* cleavage assay, cells loaded with GzmK and PJ were lysed with 0.5% Nonidet P-40 lysis buffer. The lysates were probed by immunoblotting.

Mitochondrial Isolation—Murine liver mitochondria were isolated as described (19). Briefly, the murine liver was homogenized in ice-cold mitochondria isolation buffer (MIB containing 250 mM mannitol, 0.5 mM EGTA, 5 mM HEPES, 0.1% BSA, and 0.1 mM phenylmethylsulfonyl fluoride, pH 7.2), and the pellets were removed after centrifugation at $600 \times g$ for 10 min at 4 °C. After centrifugation at $10{,}000 \times g$ for 10 min at 4 °C, the mitochondria pellet was resuspended in 4 ml of MIB and loaded onto a continuous Percoll gradient that consisted of 30% Percoll, 225 mM mannitol, 25 mM HEPES, 0.5 mM EGTA, and 0.1% BSA (pH 7.2). The suspension/gradient was centrifuged at $40{,}000 \times g$ for 1 h at 4 °C. The mitochondria were abstracted from the brownish band at 1.10 g/ml with a pipette. Then the mitochondrial pellets were washed with MIB by centrifugation at $6300 \times g$ for 10 min at 4 °C. The mitochondria were resuspended in the buffer containing 400 mM mannitol, 10 mM KH_2PO_4, 50 mM Tris-HCl (pH 7.2) with 1 mg/ml BSA.

Cytochrome c Release—Murine mitochondria were incubated with GzmK or GzmB in the presence or absence of recombinant Bid in a final volume of 50-μl reaction buffer (220 mM mannitol, 68 mM sucrose, 20 mM HEPES-KOH, pH 7.5, 10 mM KCl, 1.5 mM $MgCl_2$, 1 mM sodium EDTA, 1 mM sodium EGTA, 1 mM dithiothreitol, and 0.1 mM phenylmethylsulfonyl fluoride) at 30 °C for 30 min. After incubation, the reaction mixture was centrifuged at $12{,}000 \times g$ for 5 min. SDS buffer (5×) was added to the supernatants and the mitochondrial pellets. The samples were boiled for 5 min and loading onto the 12% SDS-PAGE for Western blot analysis using cyt *c* antibody.

RESULTS

GzmK Targets Mitochondria—We previously demonstrated GzmK induces rapid caspase-independent cell death with externalization of phosphatidylserine, nuclear morphological changes, and single-stranded DNA nicks (9). GzmK-induced death is through targeting all the three GzmA substrates of the SET complex, including SET, Ape1, and HMG2 (17, 20–22).

We compared delivery reagents for loading granzymes into the intact cells and found the cationic lipid reagent PJ can substitute for perforin or Ad to transport granzymes into target cells (9, 23). Granzymes loaded with PJ induce similar kinetics of death by loading with perforin or Ad. Mitochondrial damage is an initial step for apoptosis. One previous study showed rat GzmK induced an increase of ROS (10). We wanted to investigate whether GzmK provokes morphological changes in mitochondria. GzmK and S-AGzmK were produced with pET26b vector in *Escherichia coli* or *Pichia pastoris* system described in our previous report (9). 1 μM GzmK was loaded with PJ into HeLa cells at 37 °C for 4 h and visualized by electronic microscopy. GzmK plus PJ treatment induced profound mitochondrial swelling with loss of cristae structure (Fig. 1). The mitochondria of mock treated cells showed normal features with a condensed state and narrow cristae, identical to the mitochondria of cells treated with S-AGzmK plus PJ or GzmK alone (Fig. 1 and not shown).

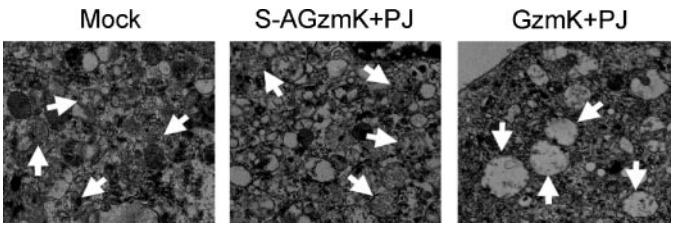

FIGURE 1. **GzmK triggers mitochondrial swelling with loss of cristae structure.** HeLa cells were incubated with 1 μM GzmK and PJ at 37 °C for 4 h and detected by a transmission electron microscopy. GzmK plus PJ-treated cells show distinct mitochondrial swelling with loss of cristae structure. The mitochondria of mock treated cells show normal features with a condensed state and narrow cristae, similar to the mitochondria of cells treated with S-AGzmK plus PJ. The normal and inflated mitochondria are indicated with *arrows*.

GzmK Causes Loss of $\Delta\Psi$—Mitochondrial functions, including protein import, ATP generation, and lipid biogenesis, are dependent on the maintenance of $\Delta\Psi$ (24). Loss of $\Delta\Psi$ is likely to contribute to the death of cells (25). To assess whether GzmK causes $\Delta\Psi$ collapse, Jurkat cells were treated with GzmK plus Ad and analyzed by FACS analysis. Cells loaded with GzmK plus Ad showed a dose-dependent decrease of $\Delta\Psi$, assayed by the change in fluorescence of the sensitive dye $DiOC_6$, which targets to the negatively charged environment of the mitochondrial matrix at a low concentration in intact cells (Fig. 2*A*). 0.5 μM GzmK started to initiate reduction of $\Delta\Psi$ within 1 h. Inactive S-AGzmK plus Ad or mock treated cells were without effect. An uncoupler of oxidative phosphorylation CCCP was used to treat cells as a positive control. GzmK-induced $\Delta\Psi$ reduction also occurred in a time-dependent manner (Fig. 2*B*). 1 μM GzmK plus Ad initiated a dramatic decrease in $\Delta\Psi$ within 1 h. By 4 h, $\Delta\Psi$ was completely collapsed. GzmK and Ad alone or S-AGzmK plus Ad had little effect. GzmK-induced $\Delta\Psi$ rupture requires enzymatic activity of GzmK.

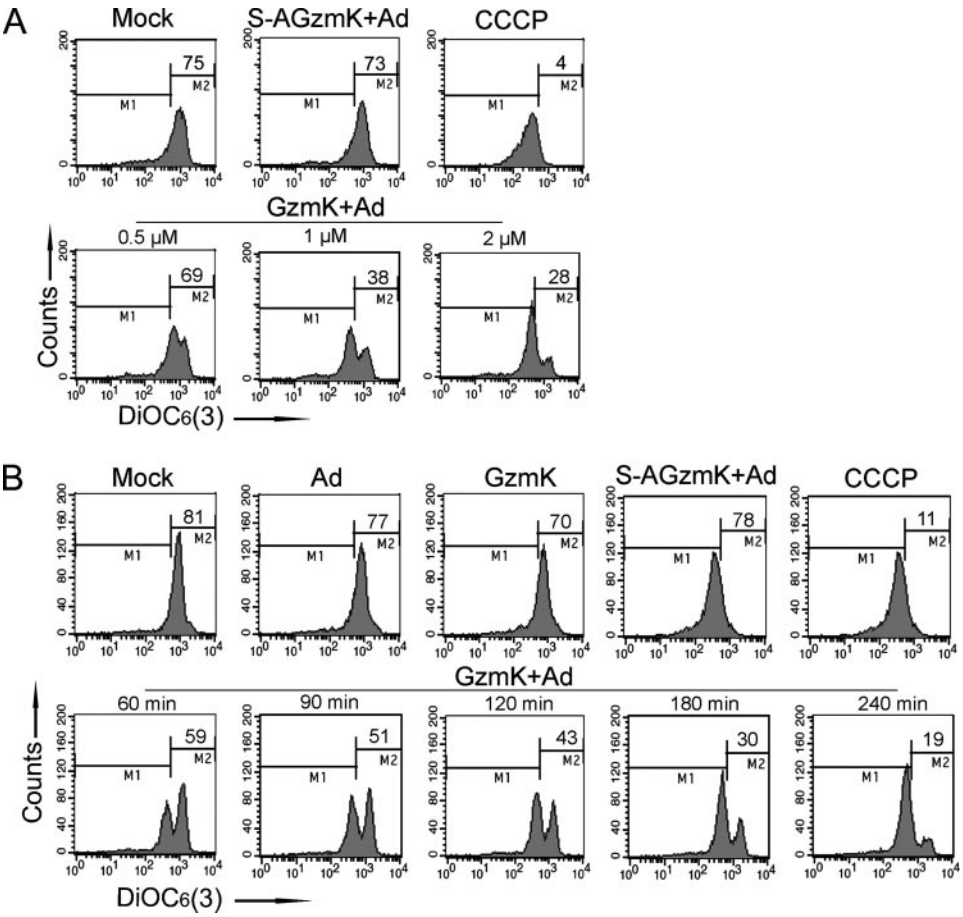

FIGURE 2. **GzmK initiates loss of mitochondrial transmembrane potential.** GzmK plus Ad induced dose- and time-dependent loss of mitochondrial $\Delta\Psi$. Jurkat cells were treated with the indicated doses of GzmK for 4 h (*A*) or 2 μM GzmK for the indicated times (*B*) in the presence of Ad (100 pfu/ml) at 37 °C. The classic uncoupler of oxidative phosphorylation carbonyl cyanide *m*-chlorophenylhydrazone (CCCP, 10 μM) was used as a positive control. Changes in mitochondrial transmembrane potential ($\Delta\Psi$) were determined by using 20 nM $DiOC_6$ (3). These data are representative of at least three independent experiments.

GzmK Triggers a Rapid Increase of Intracellular ROS—ROS have been proposed as critical regulators of apoptosis (12, 26). Superfluous ROS cause mitochondrial damage as well as nuclear DNA damage. Mitochondria are the major source of intracellular ROS (27). ROS can be generated after damage to the mitochondrial inner membrane accompanying the permeability transition, which may be one route for releasing proapoptotic factors from the intramembrane space (28). To detect ROS accumulation in GzmK-induced death, Jurkat cells were treated with GzmK plus Ad as measured by detection of the conversion of hydroethidine (HE) to fluorescent ethidium. 0.2 μM GzmK began to trigger ROS production within 50 min of treatment as seen by the increase in mean fluorescence intensity of the ROS indicator dye (Fig. 3*A*). GzmK augmented ROS generation with the increasing

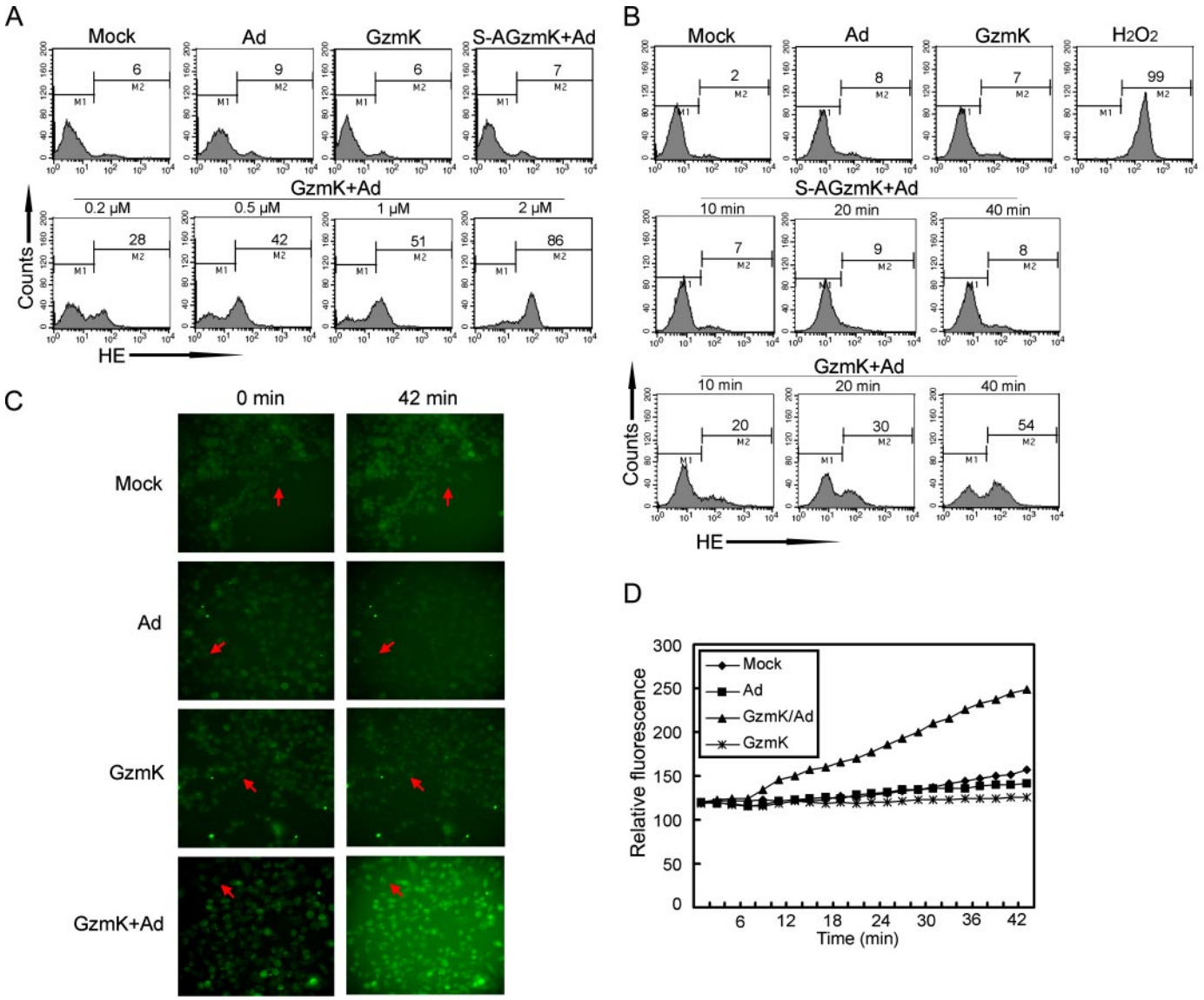

FIGURE 3. **GzmK induces ROS production.** *A* and *B*, GzmK induced ROS accumulation in a dose- and time-dependent manner. Jurkat cells were incubated with GzmK plus Ad in the indicated concentrations for 1 h or 1 μM GzmK at the indicated times, then stained with HE through analysis by flow cytometry. H_2O_2 treatment was used as a positive control. *C* and *D*, kinetics of GzmK-induced ROS production at a single cell level. HeLa cells stained with 2′,7′-dichlorofluorescin diacetate (DCF-DA) were treated with GzmK plus Ad, and followed by a time-lapse fluorescence microscopy. Images were captured every 2 min. 0 min and 42 min time intervals show the representative process of ROS increase (*C*). The *curves* represent the dynamics of ROS increase in the cells selected with *arrows* (*D*). The data are representative of three independent experiments.

concentrations. 2 μM GzmK reached a high peak for ROS production (mean fluorescence intensity, 86). ROS accumulate rapidly after GzmK treatment. Within 10 min, GzmK began to generate ROS, and ROS increased over time (Fig. 3*B*). GzmK, Ad alone, or S-AGzmK with Ad at the same time points all had comparable levels. H_2O_2-treated cells were used as a positive control. To further verify ROS generation induced by GzmK, time-lapse microscopy was used to visualize ROS production at a single cell level. HeLa cells loaded with GzmK and Ad appeared to have strong fluorescence staining (Fig. 3*C*). GzmK, Ad alone, or mock treated cells were undetectable. For detection of ROS generation, one cell was chosen and photographed every 2 min, as depicted by the *arrow*. ROS began to produce early on and increased over time, which was consistent with the above observations by FACS.

Blockade of ROS Production Inhibits GzmK-induced Cell Death—We next wanted to detect whether reagents that react with oxidative intermediates can decrease GzmK-induced ROS. The antioxidant NAC or superoxide scavenger sodium 4,5-dihydroxybenzene 1,3-disulfonate (Tiron) pretreatment inhibited GzmK-induced ROS accumulation (Fig. 4*A*). This is consistent with the observations of GzmA by Martinvalet *et al.* (15). Even high concentrations of NAC and Tiron we used were nontoxic as determined for each reagent through staining by Annexin V and propidium iodide (not shown). To further determine the consequence of ROS on cell death, Jurkat cells were preincubated with 4 mM NAC or 50 mM Tiron before being loading with GzmK by Ad, and cell death was analyzed by Annexin V or Hoechst staining. NAC treatment can inhibit GzmK-induced death (Annexin V+ cells: 22 ± 2% *versus* 54 ±

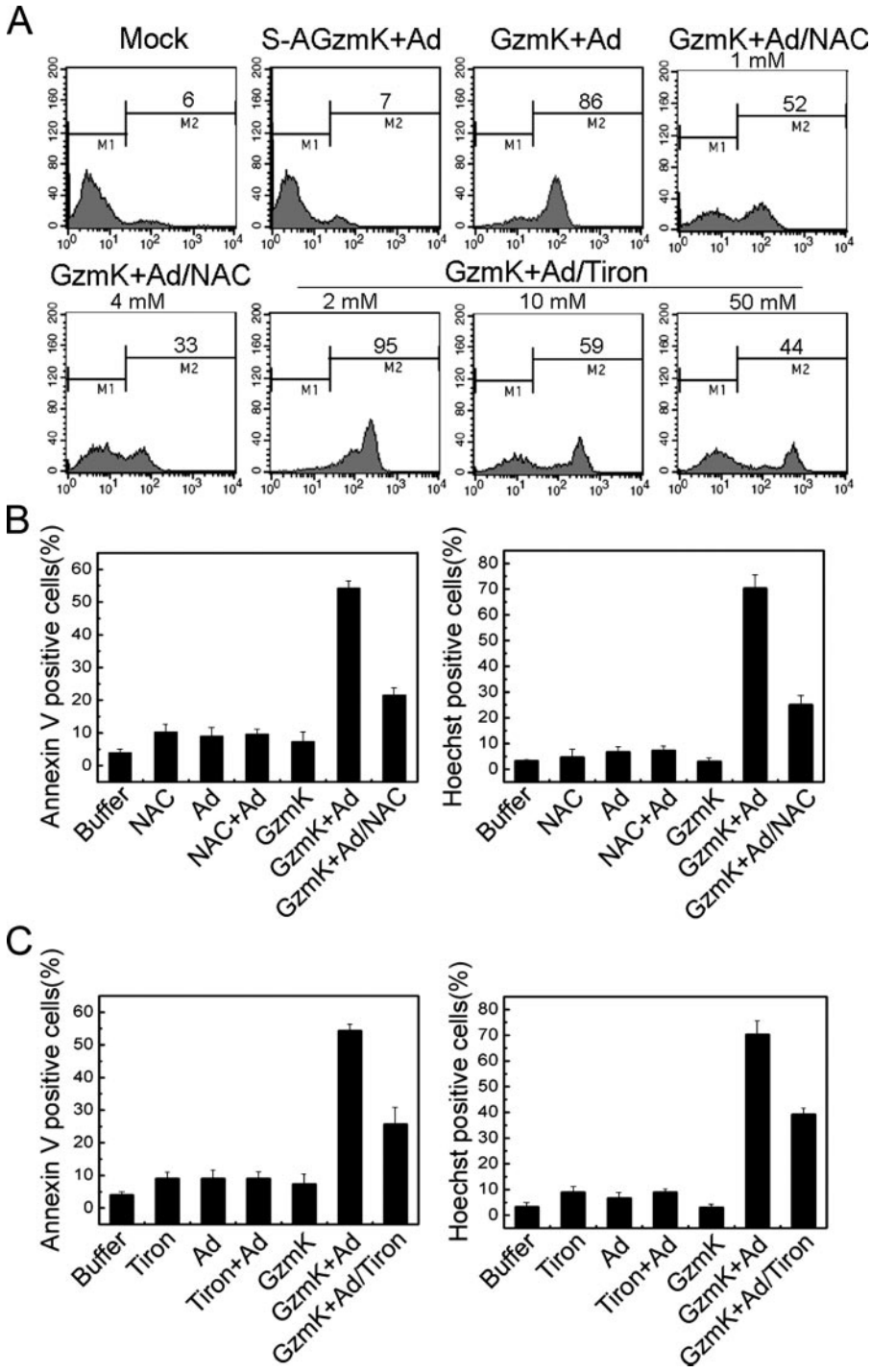

FIGURE 4. **Inhibiting ROS accumulation protects target cells from GzmK-induced death.** *A*, GzmK-induced ROS increase can be inhibited by the antioxidant NAC and free radical scavenger Tiron. NAC and Tiron inhibited GzmK-induced ROS generation in a dose-dependent manner. Data are representative of three independent experiments. *B*, Jurkat cells or Jurkat cells pretreated with 4 mM NAC were incubated with GzmK, Ad, or GzmK plus Ad for 4 h at 37 °C and stained by Annexin V or Hoechst. *C*, Jurkat cells or Jurkat cells pretreated with 50 mM Tiron were analyzed as above.

2.1%, $p < 0.01$; Hoechst staining: 25 ± 3.6% *versus* 70 ± 5.1%, $p < 0.01$) (Fig. 4*B*). Tiron treatment gave similar results (Annexin V+ cells: 22% ± 2% *versus* 54 ± 2.1%, $p < 0.01$; Hoechst staining: 25 ± 3.6% *versus* 70 ± 5.1%, $p < 0.01$) (Fig. 4*C*). Similar results were found for propidium iodide staining (data not shown). Six control groups were used: GzmK, Ad, NAC, Tiron alone, NAC plus Ad, or Tiron plus Ad. These groups resulted in comparable cell death.

GzmK Directly Processes Bid to Produce Its Active Form tBid in Its Recombinant or Native Form of Lysates and Intact Cells—Bid is a BH3-only protein of the Bcl-2 family that plays an important role in mitochondria-dependent apoptosis. Undergoing apoptosis, Bid can be processed to a truncated Bid (tBid) that potently attacks the outer mitochondrial membrane to initiate release of cyt *c* and other proapoptotic factors (19, 29). To investigate whether Bid is processed by GzmK, 0.5 μM rBid was incubated with different concentrations of GzmK and probed by anti-Bid antibody. Bid began to degrade at 0.5 μM GzmK (Fig. 5*A*). The full-length Bid was completely processed at a high concentration of 2 μM GzmK. By 30 min, Bid started to degrade after GzmK treatment and was completely hydrolyzed within 4 h. Even with high concentration of 2 μM S-AGzmK, Bid was uncleaved. To assess whether GzmK degrades native Bid, Jurkat cell lysates (2×10^5 cell equivalents) were incubated with different doses of GzmK. Bid was degraded by GzmK in a dose-dependent fashion (Fig. 5*B*). The same blot was stripped and probed with β-actin. β-Actin was unchanged as a negative control. After 2 h, Bid was dramatically degraded by 2 μM GzmK and almost completely processed by 4 h. Similar results were obtained in HeLa cells (data not shown). To further verify Bid processing is physiologically relevant, Jurkat cells were treated with 1 μM GzmK in the presence of PJ. Cytosolic Bid degradation occurred after 2 h (Fig. 5*C*). tBid production increased over time. The size of tBid produced by GzmK was similar to that processed by GzmB. Cells loaded with GzmB showed stronger enzymatic activity for Bid cleavage than GzmK. S-AGzmK was without effect. β-Actin was unchangeable at all time points as a loading control.

GzmK Induces cyt c and EndoG Release in a Bid-dependent Way—cyt c release from mitochondria appears to be an early event during apoptosis induced by a variety of stimuli (30, 31).

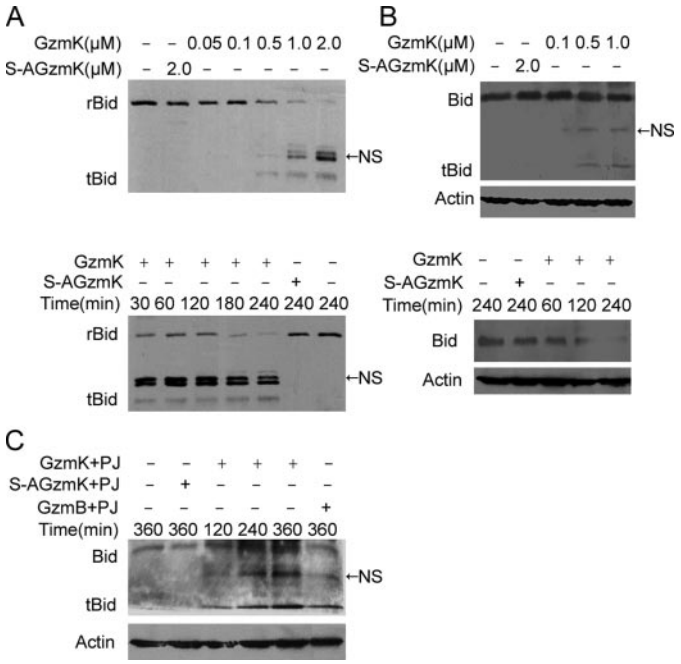

FIGURE 5. **GzmK cleaves Bid in its recombinant and its native form of lysates or intact cells.** *A*, rBid was degraded by GzmK in a dose- and time-dependent fashion. 0.5 μM rBid was incubated at 37 °C for the indicated times with different concentrations of GzmK or S-AGzmK. Reactions were stopped by 5× SDS loading buffer and analyzed by immunoblotting. *NS* represents a nonspecific band. *B*, GzmK cleaves native Bid in cell lysates. Jurkat cells (2×10^5 equivalents) were treated with GzmK and PJ at 37 °C in the indicated concentrations and times. Bid was probed as above. β-Actin was unchanged as a loading control. Similar results were obtained in HeLa cell lysates (not shown). *C*, GzmK cleaves Bid in intact cells. Jurkat cells were treated for the indicated times at 37 °C GzmK or S-AGzmK plus PJ. The whole cell lysates were analyzed by immunoblotting. GzmB plus PJ was used as a positive control. β-Actin was used as a loading control.

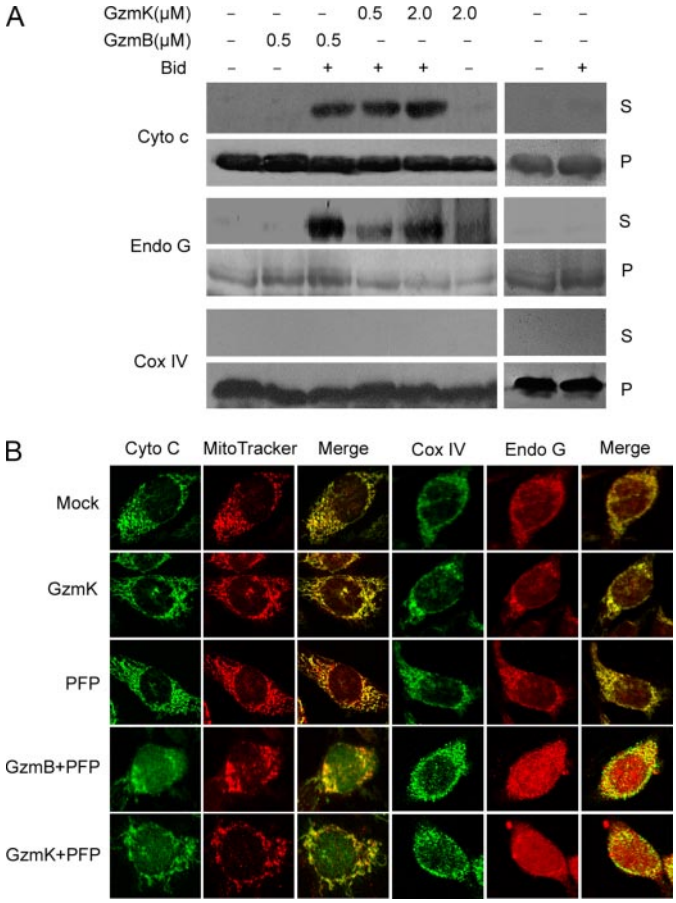

FIGURE 6. **GzmK induces cyt *c* and EndoG release.** *A*, isolated murine liver mitochondria were incubated in the indicated concentrations of GzmK in the presence or absence of rBid at 37 °C for 30 min. rBid- or GzmB plus rBid-treated mitochondria were used as controls. cyt *c* and EndoG released into the supernatants (*S*) or that remaining in mitochondria (*P*) were detected by immunoblotting. CoxIV was used as the fractionation control. These data are representative of three separate experiments. *B*, cyt *c* and EndoG release were confirmed in GzmK-loaded intact HeLa cells by confocal microscopy. cyt *c* and EndoG released quickly from mitochondria in HeLa cells after GzmK loading with PFP at 37 °C for 2 h. GzmB plus PFP was used as a positive control. cyt *c* and CoxIV staining (*green fluorescence*) is shown at the *left*, MitoTracker staining (*red*) is in the *middle*, and the *merged images* are at the *right*.

Cytosolic cyt *c*, together with Apaf-1 and procaspase-9, in an ATP-dependent manner, forms apoptosome, which causes caspase activation that orchestrates the biochemical execution of cells (32, 33). EndoG is a proapoptotic DNase that is released from mitochondria and translocates to the nucleus where it damages chromatin DNA without caspase activation during apoptosis, which represents a caspase-independent apoptotic pathway initiated from the mitochondria (34). We next wanted to investigate whether GzmK initiates the release of cyt *c* and other proapoptotic factors and whether these events are Bid-dependent. Murine liver mitochondria were isolated and treated with GzmK in the presence or absence of rBid at 37 °C for 30 min. In the presence of rBid, GzmK induced cyt *c* and EndoG release in a dose-dependent manner (Fig. 6*A*). Without rBid, even high concentration of 2 μM GzmK did not cause release of cyt *c* and EndoG. cyt *c* and EndoG release induced by GzmB also required rBid presence, which is consistent with previous reports (35, 36). cyt *c* release by 0.5 μM GzmK treatment was comparable to that of the same molar GzmB, whereas EndoG release by 0.5 μM GzmB treatment was much higher than the same molar GzmK treatment. rBid alone did not cause the release of cyt *c* and other proapoptotic factors from mitochondria. These data are representative of at least three separate experiments. CoxIV, a matrix protein of mitochondria, was used for fractionation controls. CoxIV was not detectable in the supernatants. GzmK can induce SMAC and AIF, and the release of SMAC and AIF was also required for the presence of rBid (data not shown). These results were further confirmed by laser scanning confocal microscopy (Fig. 6*B*). GzmK loading with PFP induced cyt *c* and EndoG release in HeLa cells. GzmK or PFP alone was without effect. GzmB plus PFP was used as a positive control. Similar results were found in GzmK-treated HeLa cells by delivery of PJ or Ad (data not shown).

DISCUSSION

It has not been defined how GzmK functions in CTL- and NK-cell induced cytolysis. Shi *et al.* (8, 37) showed that rat GzmK induces DNA fragmentation without nuclear morphological changes after GzmK loading with perforin and is considered as a slowing granzyme. The same group also demonstrated GzmK disrupts $\Delta\Psi$ but does not initiate release of cyt *c* (10). We previously showed that human GzmK induces rapid cell death without caspase activation (9). The features of death are characterized by rapid externalization of phosphatidylserine, nuclear morphological changes, and single-stranded DNA

nicks, which are reminiscent of the alternate tryptase GzmA. Moreover, GzmK targets all three GzmA substrates of the SET complex, such as SET, Ape1/Ref-1, and HMG2, in the same proteolytic patterns as GzmA (9, 20–22). GzmK and -A are two tryptase among all the granzymes and linked together on the same chromosome of mice and humans. Therefore, GzmK might share redundancy with GzmA. The Lieberman group (15) showed ROS is critical for the distinct caspase-independent cell death pathway triggered by GzmA. GzmA initiates mitochondrial damage with a rapid increase in ROS and loss of $\Delta\Psi$. GzmA does not cleave Bid or induce release of mitochondrial proapoptotic molecules. In this study we found GzmK can also provoke rapid ROS generation and collapse of $\Delta\Psi$. But GzmK directly cleaves Bid to generate its active form tBid that disrupts the outer mitochondrial membrane leading to the release of cyt *c* and EndoG that is different from GzmA.

Mitochondria play a central role in both the caspase-dependent and -independent death pathway (30). They contain a number of proapoptotic proteins, such as cyt *c*, SMAC, high temperature-requirement protein A2, AIF, and EndoG, which are released into the cytosol undergoing apoptosis. The release of proapoptotic factors from mitochondria is due to the rupture of mitochondrial integrity. These events are initiated by the opening of the PTP (13). Opening of PTP triggers an increase of inner membrane permeability to ions and solutes, followed by net water influx toward the mitochondrial matrix, swelling of the organelle, and physiological disruption of its outer membrane, with the consequent release of proteins to the intermembrane space. Increase of ROS and loss of $\Delta\Psi$ are indicative of mitochondrial dysfunction, hallmarks of apoptotic mitochondrial damage (12). It is postulated that ROS and $\Delta\Psi$ collapse are early events in apoptosis that involve the opening by PTP of the inner mitochondrial membrane (10, 38). We showed that GzmK triggers rapid ROS production and loss of $\Delta\Psi$. Our data suggest that GzmK damages the inner mitochondrial membrane thus resulting in mitochondrial solutes to the intermembrane space.

Whether generation of ROS is critical to apoptosis or only a side effect of mitochondrial dysfunction has not been well defined. ROS induce the opening of PTP through oxidation-dependent mechanisms and are potent inducers of apoptosis (12, 39). Lieberman's group (15) showed that ROS is critical in GzmA-induced caspase-independent death. ROS generation induced by GzmA is not inhibited by Bcl-2 overexpression or by pan caspase inhibitors. We found that GzmK can initiate rapid ROS generation and confirmed this at a single cell level. Both the antioxidant NAC and the superoxide scavenger Tiron blocked ROS production, which protected cells from GzmK-induced death. By contrast, Martinvalet *et al.* (15) reported that NAC is less effective than Tiron at neutralizing ROS and is unable to protect GzmA-induced death. We previously showed that GzmK can cleave Ape1/Ref-1 leading to disruption of its redox function as GzmA (9, 22). A primary function of Ape1/Ref-1 is maintaining reduced thiols and DNA binding of transcription factors, such as AP-1 and NF-κB. Ape1/Ref-1 can inhibit intracellular ROS accumulation. We found that GzmK can degrade tumor suppressor p53.[4] A recent study showed that p53 protects genome stability from oxidation by ROS (40). Down-regulation of p53 results in excessive oxidation of DNA that is prevented by NAC treatment. Dietary supplementation with NAC prevents frequent lymphomas characteristic of p53-deficient mice.

cyt *c* release from mitochondria has been defined as an important event in the activation of downstream caspases and apoptosis (31). Once released to the cytosol, cyt *c* acts as a cofactor in conjunction with Apaf-1, procaspase 9, and ATP/dATP to form an active holoenzyme that processes and activates downstream caspase 3 (30, 32, 33). The signals to induce cyt *c* release are often propagated through proapoptotic Bcl-2 family members. Translocation from the cytoplasm to mitochondria during apoptosis has been reported for Bid, Bax, Bak, Bad, and Bim (19, 41–45). These proteins are inactive in the cytoplasm and are translocated to the mitochondria after a death signal. Following Fas ligation and recruitment of Fas-associated death domain to the trimeric receptor complex, caspase 8 is activated and then degrades cytosolic Bid to tBid, which translocates to mitochondria to cause the release of cyt *c* (19). GzmB directly cleaves Bid to produce a 14-kDa GzmB-truncated Bid (called gtBid), which is different from caspase 8-truncated 15-kDa tBid (36). gtBid recruits Bax to mitochondria through a caspase-independent mechanism where it is integrated into the mitochondrial membrane and initiates cyt *c* release. We showed here that Bid is processed by GzmK, which appears to have the same pattern as GzmB. GzmK-truncated Bid might mimic gtBid to recruit Bax leading to caspase-independent mechanism of mitochondrial damage, which is different from GzmA. Moreover, GzmK can induce the release of other proapoptotic molecules, including EndoG, SMAC, and AIF, which enhance GzmK-induced death.

Acknowledgments—We thank L. Wang, Q. X. Zhang, Q. Hou, H. X. Lu, G. Q. Hua, W. Xu, Y. Y. Chen, C. C. Liu, and Y. L. Xu for their technical support; Dr. J. Trapani for providing the recombinant mouse perforin; Dr. X. Wang for providing Bid, SMAC, AIF, and EndoG antibodies; and Dr. C. Weng for providing rBid protein.

REFERENCES

1. Hameed, A., Lowrey, D. M., Lichtenheld, M., and Podack, E. R. (1988) *J. Immunol.* **141,** 3142–3147
2. Grossman, W. J., Revell, P. A., Lu, Z. H., Johnson, H., Bredemeyer, A. J., and Ley, T. J. (2003) *Curr. Opin. Immunol.* **15,** 544–552
3. Shresta, S., Goda, P., Wesselschmidt, R., and Ley, T. J. (1997) *J. Biol. Chem.* **272,** 20236–20244
4. Carter, C. R., Sayers, T. J., Wiltrout, R. H., Turcovski-Corrales, S. M., and Taub, D. D. (1996) *Cell. Immunol.* **172,** 235–245
5. Davis, J. E., Smyth, M. J., and Trapani, J. A. (2001) *Eur. J. Immunol.* **31,** 39–47
6. Bratke, K., Kuepper, M., Bade, B., Virchow, J. C., Jr., and Luttmann, W. (2005) *Eur. J. Immunol.* **35,** 2608–2616
7. Bade, B., Lohrmann, J., Ten Brinke, A., Wolbink, A. M., Wolbink, G. J., Berge, I. J., Virchow, J. C., Jr., Luttmann, W., and Hack, C. E. (2005) *Eur. J. Immunol.* **35,** 2940–2948
8. Shi, L., Kraut, R. P., Aebersold, R., and Greenberg, A. H. (1992) *J. Exp. Med.* **175,** 553–566

[4] T. Zhao, H. Zhang, Y. Guo, and Z. Fan, unpublished data.

9. Zhao, T., Zhang, H., Guo, Y., Zhang, Q., Hua, G., Lu, H., Hou, Q., Liu, H., and Fan, Z. (2006) *Cell Death Differ.* **14,** 489–499
10. MacDonald, G., Shi, L., Vande Velde, C., Lieberman, J., and Greenberg, A. H. (1999) *J. Exp. Med.* **189,** 131–144
11. Chipuk, J. E., and Green, D. R. (2005) *Nat. Rev. Mol. Cell. Biol.* **6,** 268–275
12. Danial, N. N., and Korsmeyer, S. J. (2004) *Cell* **116,** 205–219
13. Bernardi, P., Petronilli, V., Di Lisa, F., and Forte, M. (2001) *Trends. Biochem. Sci.* **26,** 112–117
14. Scorrano, L., Oakes, S. A., Opferman, J. T., Cheng, E. H., Sorcinelli, M. D., Pozzan, T., and Korsmeyer, S. J. (2003) *Science* **300,** 135–139
15. Martinvalet, D., Zhu, P., and Lieberman, J. (2005) *Immunity* **22,** 355–370
16. Fan, Z., and Zhang, Q. (2005) *Cell. Mol. Immunol.* **2,** 259–264
17. Lieberman, J., and Fan, Z. (2003) *Curr. Opin. Immunol.* **15,** 553–559
18. Barry, M., Heibein, J. A., Pinkoski, M. J., Lee, S. F., Moyer, R. W., Green, D. R., and Bleackley, R. C. (2000) *Mol. Cell. Biol.* **20,** 3781–3794
19. Luo, X., Budihardjo, I., Zou, H., Slaughter, C., and Wang, X. (1998) *Cell* **94,** 481–490
20. Fan, Z., Beresford, P. J., Oh, D. Y., Zhang, D., and Lieberman, J. (2003) *Cell* **112,** 659–672
21. Fan, Z., Beresford, P. J., Zhang, D., and Lieberman, J. (2002) *Mol. Cell. Biol.* **22,** 2810–2820
22. Fan, Z., Beresford, P. J., Zhang, D., Xu, Z., Novina, C. D., Yoshida, A., Pommier, Y., and Lieberman, J. (2003) *Nat. Immunol.* **4,** 145–153
23. Lu, H., Hou, Q., Zhao, T., Zhang, H., Zhang, Q., Wu, L., and Fan, Z. (2006) *J. Immunol.* **177,** 1171–1178
24. Voisine, C., Craig, E. A., Zufall, N., von Ahsen, O., Pfanner, N., and Voos, W. (1999) *Cell* **97,** 565–574
25. Ricci, J. E., Gottlieb, R. A., and Green, D. R. (2003) *J. Cell Biol.* **160,** 65–75
26. Balaban, R. S., Nemoto, S., and Finkel, T. (2005) *Cell* **120,** 483–495
27. Esposito, L. A., Melov, S., Panov, A., Cottrell, B. A., and Wallace, D. C. (1999) *Proc. Natl. Acad. Sci. U. S. A.* **96,** 4820–4825
28. Green, D. R., and Kroemer, G. (2004) *Science* **305,** 626–629
29. Li, H., Zhu, H., Xu, C. J., and Yuan, J. (1998) *Cell* **94,** 491–501
30. Jiang, X., and Wang, X. (2004) *Annu. Rev. Biochem.* **73,** 87–106
31. Yang, J., Liu, X., Bhalla, K., Kim, C. N., Ibrado, A. M., Cai, J., Peng, T. I., Jones, D. P., and Wang, X. (1997) *Science* **275,** 1129–1132
32. Li, P., Nijhawan, D., Budihardjo, I., Srinivasula, S. M., Ahmad, M., Alnemri, E. S., and Wang, X. (1997) *Cell* **91,** 479–489
33. Zou, H., Henzel, W. J., Liu, X., Lutschg, A., and Wang, X. (1997) *Cell* **90,** 405–413
34. Li, L. Y., Luo, X., and Wang, X. (2001) *Nature* **412,** 95–99
35. Alimonti, J. B., Shi, L., Baijal, P. K., and Greenberg, A. H. (2001) *J. Biol. Chem.* **276,** 6974–6982
36. Heibein, J. A., Goping, I. S., Barry, M., Pinkoski, M. J., Shore, G. C., Green, D. R., and Bleackley, R. C. (2000) *J. Exp. Med.* **192,** 1391–1402
37. Shi, L., Kam, C. M., Powers, J. C., Aebersold, R., and Greenberg, A. H. (1992) *J. Exp. Med.* **176,** 1521–1529
38. Zamzami, N., Susin, S. A., Marchetti, P., Hirsch, T., Gomez-Monterrey, I., Castedo, M., and Kroemer, G. (1996) *J. Exp. Med.* **183,** 1533–1544
39. Petronilli, V., Costantini, P., Scorrano, L., Colonna, R., Passamonti, S., and Bernardi, P. (1994) *J. Biol. Chem.* **269,** 16638–16642
40. Sablina, A. A., Budanov, A. V., Ilyinskaya, G. V., Agapova, L. S., Kravchenko, J. E., and Chumakov, P. M. (2005) *Nat. Med.* **11,** 1306–1313
41. Bouillet, P., Metcalf, D., Huang, D. C., Tarlinton, D. M., Kay, T. W., Kontgen, F., Adams, J. M., and Strasser, A. (1999) *Science* **286,** 1735–1738
42. Datta, S. R., Dudek, H., Tao, X., Masters, S., Fu, H., Gotoh, Y., and Greenberg, M. E. (1997) *Cell* **91,** 231–241
43. Goping, I. S., Gross, A., Lavoie, J. N., Nguyen, M., Jemmerson, R., Roth, K., Korsmeyer, S. J., and Shore, G. C. (1998) *J. Cell Biol.* **143,** 207–215
44. Griffiths, G. J., Dubrez, L., Morgan, C. P., Jones, N. A., Whitehouse, J., Corfe, B. M., Dive, C., and Hickman, J. A. (1999) *J. Cell Biol.* **144,** 903–914
45. Zinkel, S. S., Hurov, K. E., Ong, C., Abtahi, F. M., Gross, A., and Korsmeyer, S. J. (2005) *Cell* **122,** 579–591